ISSCR

OPEN ACCESS

A DGCR8-Independent Stable MicroRNA Expression Strategy Reveals Important Functions of miR-290 and miR-183–182 Families in Mouse Embryonic Stem Cells

Xi-Wen Wang,[1] Jing Hao,[1] Wen-Ting Guo,[1] Le-Qi Liao,[1] Si-Yue Huang,[1] Xiangpeng Guo,[2] Xichen Bao,[2] Miguel A. Esteban,[2] and Yangming Wang[1,*]

[1]Beijing Key Laboratory of Cardiometabolic Molecular Medicine, Institute of Molecular Medicine, Peking University, Beijing 100871, China
[2]Laboratory of RNA, Chromatin, and Human Disease, Key Laboratory of Regenerative Biology and Guangdong Provincial Key Laboratory of Stem Cells and Regenerative Medicine, Guangzhou Institutes of Biomedicine and Health, Chinese Academy of Sciences, Guangzhou 510530, China
*Correspondence: yangming.wang@pku.edu.cn
https://doi.org/10.1016/j.stemcr.2017.08.027

SUMMARY

Dgcr8 knockout cells provide a great means to understand the function of microRNAs (miRNAs) *in vitro* and *in vivo*. Current strategies to study miRNA function in *Dgcr8* knockout cells depend on transient transfection of chemically synthesized miRNA mimics, which is costly and not suitable for long-term study and genetic selection of miRNA function. Here, we developed a cost-effective DGCR8-independent stable miRNA expression (DISME) strategy based on a short hairpin RNA vector that can be precisely processed by DICER. Using DISME, we found that miR-294 promoted the formation of meso-endoderm lineages during embryonic stem cell differentiation. Furthermore, DISME allowed for a pooled screen of miRNA function and identified an miR-183–182 cluster of miRNAs promoting self-renewal and pluripotency in mouse embryonic stem cells. Altogether, our study demonstrates that DISME is a robust and cost-effective strategy that allows for long-term study and genetic selection of miRNA function in a *Dgcr8* knockout background.

INTRODUCTION

MicroRNAs (miRNAs) are a class of small noncoding RNAs ~22 nucleotides in length. As one of the most important classes of post-transcriptional regulators, they are predicted to fine-tune the expression of hundreds of mRNAs in mammals (Bartel, 2009; Jonas and Izaurralde, 2015). Numerous reports have demonstrated an essential function of miRNAs in a variety of biologic processes, including development (Amin et al., 2015; Hasuwa et al., 2013; Parchem et al., 2015), regeneration (Tian et al., 2015), and cancer (He et al., 2005; Lujambio and Lowe, 2012). Typically, miRNAs are generated by two sequential cleavages of pri-miRNAs, first by a microprocessor consisting of DROSHA and DGCR8 in nucleus (Denli et al., 2004; Ha and Kim, 2014; Han et al., 2006), then by DICER1 in cytoplasm (Hammond, 2005; Hutvagner et al., 2001). Once loaded into the RNA-induced silencing complex, miRNAs bind their targets through partial complementarity with the 3′ UTR of their target mRNAs (Chendrimada et al., 2005). The second to the eighth nucleotide at the 5′ end of miRNA is essential for the recognition of its mRNA targets, which is termed the "seed sequence" (Lewis et al., 2003).

Tackling the function of miRNAs is often impeded by the extraordinary redundancy among miRNAs. Mammalian genomes encode thousands of miRNAs, and many of them share identical or similar seed sequences, therefore acting redundantly to regulate gene expression (Fischer et al., 2015; Olive et al., 2015). For example, the let-7 family has 13 different members encoded by 10 loci in the mouse genome. In addition, miRNAs with different seed sequences could also repress the same mRNAs or even different mRNAs to exert similar functions, which makes up additional layers of redundancy (Fischer et al., 2015; Olive et al., 2015). To solve the redundancy issue, we and others have constructed *in vitro* and *in vivo* miRNA deficient models that do not express any canonical mature miRNAs by knocking out *Dgcr8* or *Dicer1* (Kanellopoulou et al., 2005; Wang et al., 2007). Recently, using *Dgcr8* knockout cells, Liu et al. (2015) found that canonical miRNAs as a whole facilitate but are not required for the reprogramming of induced pluripotent stem cells. Typically, for specific phenotypic defects found in *Dgcr8* or *Dicer1* knockout cells, screens with a library of chemically synthetic miRNA mimics are then designed to identify miRNAs that can rescue corresponding defects (Wang et al., 2008). Using this strategy, we and others have identified many miRNAs that play important functions in controlling the cell cycle, metabolism, pluripotency, and differentiation of embryonic stem cells (ESCs) (Cao et al., 2015; Gu et al., 2016; Ma et al., 2015; Sinkkonen et al., 2008; Wang et al., 2008, 2013). However, due to the transient nature of transfection of miRNA mimics, studies on the long-term function of miRNAs are limited. In addition, the transfection efficiency of miRNA mimics varies a lot in different cell types, therefore limiting this strategy to only a subset of cells. More importantly, genetic selection cannot be designed based on miRNA mimics, which makes the identification of functional miRNAs a laborious and expensive procedure.

CrossMark

Therefore, a stable miRNA expression system in *Dgcr8* knockout cells will accelerate the functional study of miRNAs and generally benefit the miRNA field.

In this study, we developed a cost-effective DGCR8-independent stable miRNA expression (DISME) strategy. We showed that DISME is generally applicable for the expression of miRNAs with different sequences. The miR-290 family of miRNAs are important for the rapid proliferation and maintenance of pluripotency in ESCs (Guo et al., 2015; Melton et al., 2010; Wang et al., 2013). We achieved high expression of miR-294 in *Dgcr8* knockout ESCs with DISME and showed that the DISME of miR-294 can efficiently rescue various defects of *Dgcr8* knockout ESCs in proliferation and differentiation. In addition, we studied the long-term function of miR-294 in the embryoid body by DISME and found that miR-294 is sufficient to promote the formation of mesoderm and endoderm lineages. More importantly, we demonstrated that DISME can be adapted for genetic selection of miRNA function and identified miR-183–182 cluster of miRNAs acting redundantly with miR-290 cluster to promote pluripotency in mouse ESCs. Therefore, DISME is a robust and cost-effective strategy that allows for long-term study and genetic selection of miRNA function in *Dgcr8* knockout cells.

RESULTS

Design of DISME
We designed a DISME strategy based on a Pol III-driven short hairpin RNA (shRNA) strategy that implements a "loop-counting" rule for the precise processing of DICER, as described previously by Gu et al. (2012) (Figure 1A). The construct begins with a guanine for Pol III recognition and ends with six uridines as a termination signal for transcription. The first to the 18th nucleotide sequence of a given miRNA is placed at the 3′ arm of shRNA to allow precise processing. We did not use the full sequence of miRNAs since the 3′ end sequence of miRNAs is not important for their function.

DISME Expresses miRNAs with Precise 5′ Ends in *Dgcr8*^{−/−} ESCs
To evaluate the universality of DISME, we chose 21 of the most abundant miRNAs expressed in mouse ESCs as candidates (Yan et al., 2017) (Table S1). A pool of plasmids containing a mixture of DISME cassettes was transfected into *Dgcr8* knockout ESCs. After brief selection with blasticidin, RNAs were extracted from the cells and small RNAs were analyzed by deep sequencing. Remarkably, we found that DISME of all miRNAs generated reads mapped to shRNA constructs (Figures 1B and 2), indicating that DGCR8 is dispensable for the processing of shRNA. More impor-

tantly, for all miRNAs except miR-7a, at least 90% of small RNA reads have 5′ ends mapped to the canonical cleavage site (Figures 1B, 2, and S1), indicating the generality of DISME in expressing miRNAs in *Dgcr8* knockout cells.

DISME of miR-294 Is Functional in *Dgcr8*^{−/−} ESCs
Next, we tested whether miRNAs expressed by DISME were functional. The miR-290 cluster encodes three miRNAs, including miR-291a-3p, miR-294, miR-295 with a seed sequence AAGUGCU, that are highly expressed and play essential functions in promoting proliferation and pluripotency in mouse ESCs (Melton et al., 2010; Wang et al., 2008). We chose miR-294 for further tests since its functions are well characterized in ESCs. To increase the expression level of miR-294, we inserted four tandem units of a U6 promoter-driven expression cassette in the same vector. We gained a cell line that expressed miR-294 at similar level as wild-type ESCs (Figure 3A). We first analyzed the expression of known direct and indirect targets of miR-294 (Cao et al., 2015; Melton et al., 2010; Wang et al., 2008, 2013) and found that all of them were essentially rescued by DISME of miR-294 in *Dgcr8* knockout ESCs to the level seen in wild-type ESCs (Figure 3B). Excitingly, miR-294 DISME cells also proliferated at a rate similar to wild-type ESCs (Figure 3C). We then tested whether DISME of miR-294 can promote the self-renewal and pluripotency of *Dgcr8*^{−/−} ESCs in the presence of differentiation-inducing miRNA let-7 (Melton et al., 2010; Wang et al., 2013). Based on colony morphology, alkaline phosphatase staining, and the expression of key pluripotency genes, the DISME of miR-294 successfully blocked let-7c-induced differentiation in *Dgcr8*^{−/−} ESCs (Figures 3D and 3E). Moreover, the DISME of miR-294 also blocked the function of other previously reported pluripotency silencing inducers, including miR-26a, miR-218, miR-199b, miR-99b, and miR-193 (Wang et al., 2013) (Figure 3F). Taken together, these data demonstrate that DISME can produce high enough levels of miRNAs that recapitulate previously identified functions of synthetic miRNA mimics.

miR-294 Promotes the Formation of Mesoderm and Endoderm Lineages in Embryoid Bodies
We previously showed that *Dgcr8*^{−/−} ESCs cannot differentiate properly during embryoid body differentiation even when more cells were added to compensate for proliferation defects (Wang et al., 2007). Interestingly, the miRNAs from the miR-290 family are continuously highly expressed in embryoid bodies for at least 8 days (Hadjimichael et al., 2016) (Figure S2A), suggesting that this family may have functions during embryoid body differentiation. Transfection of miRNA mimics into embryoid body is apparently impractical, so we investigated the function of miR-294 in embryoid body differentiation using DISME.

Figure 1. Design Strategy for Stable miRNA Overexpression in *Dgcr8*$^{-/-}$ Cells

(A) Schematic representation of the U6-driven DISME miRNA used in this study. Sequences for DISME of miR-103 and miR-182 are shown. Pol III, RNA polymerase III; miRNA strand, light blue; passenger strand, orange.

(B) The distribution of small RNA-seq reads across the DISME hairpins of miR-103 and miR-182. The y axis indicates the read count at each nucleotide position.

Interestingly, large cysts were readily observed in both wild-type and miR-294 DISME but not *Dgcr8*$^{-/-}$ ESCs (Figure 4A). The yolk-sac-like cyst structure indicated that miR-294 may promote ESC differentiation into mesoderm and endoderm. Indeed, qPCR analysis of endoderm (*Hnf4*, *Sox17*, *Foxa2*, and *Afp*) and mesoderm (*T*, *Mix1l*, *Gata4*, and *Cdx2*) markers showed that miR-294 partially rescued the defects of *Dgcr8*$^{-/-}$ ESCs in differentiation into these lineages (Figures 4B and 4C). However, qPCR analysis of ectoderm (*Sox3*, *Pax6*, *Tubb3*, and *Nestin*) markers indicate that miR-294 has little impact (comparing Dg8KO and Dg8KO-miR-294) on ectoderm differentiation (Figure 4D). These data indicate that miR-294 initiated meso- and endoderm differentiation by facilitating the exit of the

Figure 2. Observed Cleavage Efficiency at the 5′ End of miRNAs from Small RNA-Seq

DISME miR-19a
5′-——G UUUGCAUAGAUUUGCACA CU C C U GCUAC C C U G
UUUC AAACGUAUCUAAACGUGU GA A C C CGAUG A C C C
99.0

DISME miR-19b
5′-——G UUUGCAUGGAUUUGCACA CU C C U GCUAC C C U G
UUUC AAACGUACCUAAACGUGU GA A C C CGAUG A C C C
99.1

DISME miR-20a
5′-——G UGCACUAUAAGCACUUUA CU C C U GCUAC C C U G
UUUC ACGUGAUAUUCGUGAAAU GA A C C CGAUG A C C C
100

DISME miR-26a
5′-——G UAUCCUGGAUUACUUGAA CU C C U GCUAC C C U G
UUUC AUAGGACCUAAUGAACUU GA A C C CGAUG A C C C
98.5

DISME miR-93
5′-——G UGCACGAACAGCACUUUG CU C C U GCUAC C C U G
UUUC ACGUGCUUGUCGUGAAAC GA A C C CGAUG A C C C
92.2

DISME miR-96
5′-——G AAAUGUGCUAGUGCCAAA CU C C U GCUAC C C U G
UUUC UUUACACGAUCACGGUUU GA A C C CGAUG A C C C
99.5

DISME miR-103
5′-——G GCCCUGUACAAUGCUGCU CU C C U GCUAC C C U G
UUUC CGGGACAUGUUACGACGA GA A C C CGAUG A C C C
99.4

DISME miR-127
5′-——G AAGCUCAGACGGAUCCGA CU C C U GCUAC C C U G
UUUC UUCGAGUCUGCCUAGGCU GA A C C CGAUG A C C C
99.6

DISME miR-130a
5′-——G CCUUUUAACAUUGCACUG CU C C U GCUAC C C U G
UUUC GGAAAAUUGUAACGUGAC GA A C C CGAUG A C C C
97.4

DISME miR-135b
5′-——G UAGGAAUGAAAAGCCAUA CU C C U GCUAC C C U G
UUUC AUCCUUACUUUUCGGUAU GA A C C CGAUG A C C C
99.2

DISME miR-142
5′-——G AAAGUAGGAAACACUACA CU C C U GCUAC C C U G
UUUC UUUCAUCCUUUGUGAUGU GA A C C CGAUG A C C C
95.6

DISME miR-182
5′-——G AGUUCUACCAUUGCCAAA CU C C U GCUAC C C U G
UUUC UCAAGAUGGUAACGGUUU GA A C C CGAUG A C C C
99.6

DISME miR-183
5′-——G AAUUCUACCAGUGCCAUA CU C C U GCUAC C C U G
UUUC UUAAGAUGGUCACGGUAU GA A C C CGAUG A C C C
99.8

DISME miR-291a
5′-——G AGGGCCUCCACUUUGAUG CU C C U GCUAC C C U G
UUUC UCCCGGAGGUGAAACUAC GA A C C CGAUG A C C C
91.3

DISME miR-292-5p
5′-——G AGAGCCCCCAGUUUGAGU CU C C U GCUAC C C U G
UUUC UCUCGGGGGUCAAACUCA GA A C C CGAUG A C C C
98.3

DISME miR-292-3p
5′-——G AAAACCUGGCGGCACUUU CU C C U GCUAC C C U G
UUUC UUUUGGACCGCCGUGAAA GA A C C CGAUG A C C C
97.5

DISME miR-293
5′-——G AUGUCACACAGUUUGAGU CU C C U GCUAC C C U G
UUUC UACAGUGUGUCAAACUCA GA A C C CGAUG A C C C
99.1

DISME miR-294
5′-——G ACAAAAGGGAAGCACUUU CU C C U GCUAC C C U G
UUUC UGUUUUCCCUUCGUGAAA GA A C C CGAUG A C C C
99.5

DISME miR-541
5′-——G CCAACAUCAGAAUCCCUU CU C C U GCUAC C C U G
UUUC GGUUGUAGUCUUAGGGAA GA A C C CGAUG A C C C
93.0

DISME miR-672
5′-——G CACAGUACACCAACCUCA CU C C U GCUAC C C U G
UUUC GUGUCAUGUGGUUGGAGU GA A C C CGAUG A C C C
99.9

Arrows and associated numbers indicate the percentage of sequences starting at the 5′ end of each miRNA relative to the total number of miRNA strand reads.

pluripotency state at early stages of differentiation. Consistent with this, miR-294 DISME promoted the silencing of naive pluripotency genes and the upregulation of primed markers during transition from naive ESC state to primed epiblast-like cell (EpiLC) state in differentiation media containing basic fibroblast growth factor (Figure S2B), although not as efficiently as observed in wild-type ESCs. Taken together, these data validated that DISME can be

Figure 3. Stable Overexpression of miR-294 by DISME Rescues the Proliferation and Self-Renewal Defects of $Dgcr8^{-/-}$ ESCs

(A) The relative expression level of DISME miR-294 compared with miR-294 in wild-type cells by miRNA qPCR. miR-183 and miR-293 are two negative controls showing that other miRNAs are not expressed in miR-294 DISME $Dgcr8^{-/-}$ ESCs. Data were normalized to 5S rRNA and then to wild-type ESCs. Shown are means ± SD, n = 3 independent experiments.

(B) qRT-PCR analysis of direct targets of miR-294 and other genes indirectly upregulated by miR-294. The β-actin gene was used as a control. For each gene, data were normalized to the mRNA level of wild-type ESCs. Shown are means ± SD, n = 3 independent experiments.

(C) Population doubling time of wild-type, $Dgcr8^{-/-}$ and DISME miR-294 rescued $Dgcr8^{-/-}$ ESCs. Shown are means ± SD, n = 4 independent experiments.

(D) Representative images of alkaline phosphatase staining of $Dgcr8^{-/-}$ and DISME miR-294 rescued $Dgcr8^{-/-}$ cells after mock or let-7c transfection.

(E) qRT-PCR for Oct4, Sox2, and Nanog for $Dgcr8^{-/-}$ and DISME miR-294 rescued $Dgcr8^{-/-}$ cells after mock or let-7c transfection. The β-actin gene was used as a control. For each gene, data were normalized to the mRNA level of mock-transfected ESCs. Shown are means ± SD, n = 3 independent experiments.

(F) qRT-PCR for *Oct4*, *Sox2*, and *Nanog* for $Dgcr8^{-/-}$ and DISME miR-294-rescued $Dgcr8^{-/-}$ cells after transfection with various differentiation-inducing miRNAs. The β-actin gene was used as a control. For each gene, data were normalized to the mRNA level of mock-transfected ESCs. Shown are means ± SD, n = 3 independent experiments.
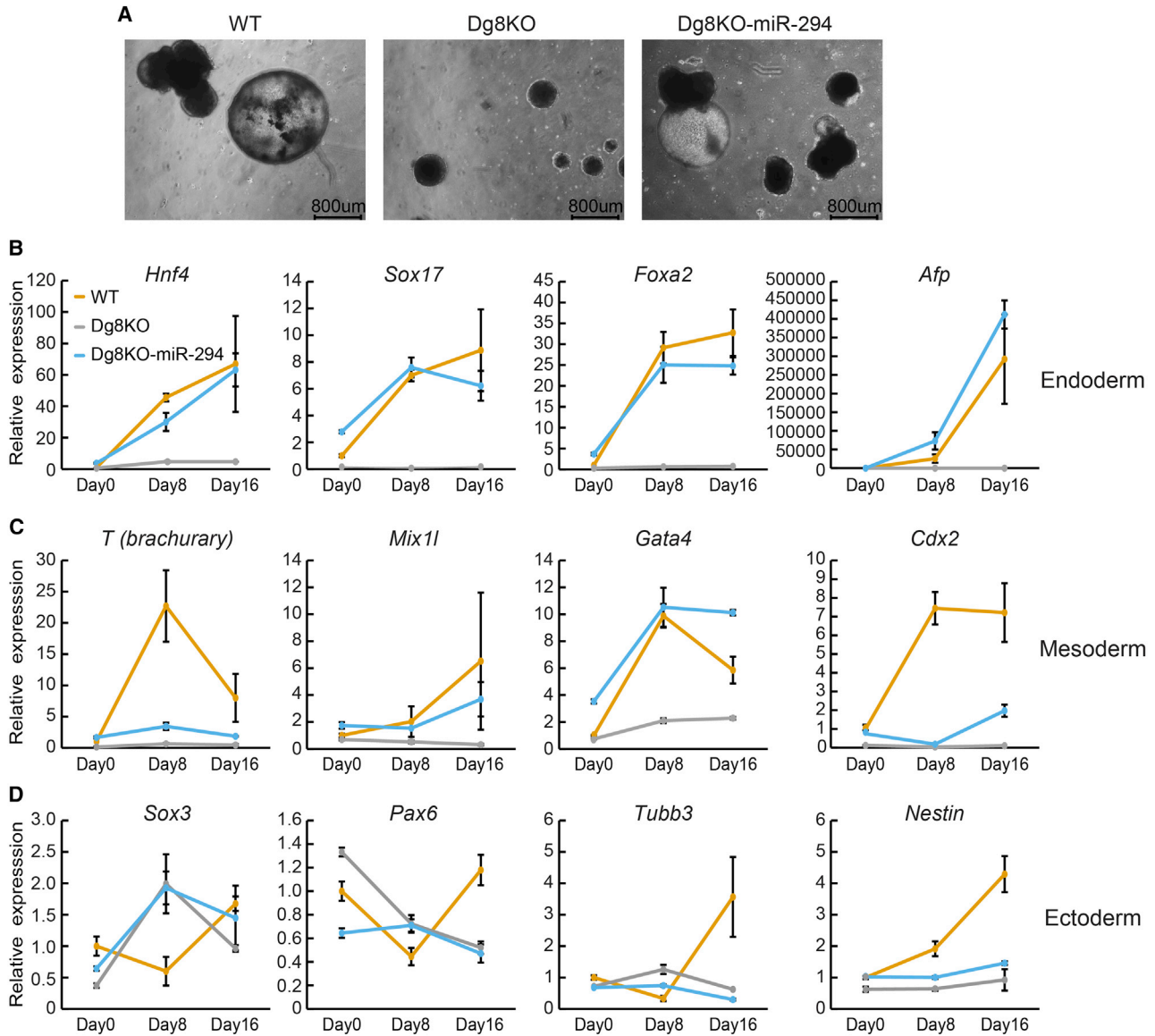
Figure 4. miR-294 Promotes the Differentiation of ESCs into Mesoderm and Endoderm Lineages

(A) Representative images of embryoid bodies for wild-type, $Dgcr8^{-/-}$, and DISME miR-294-rescued $Dgcr8^{-/-}$ ESCs.

(B–D) qRT-PCR analysis of representative markers of (B) endoderm (*Hnf4*, *Sox17*, *Afp*, *Foxa2*), (C) mesoderm (*T*, *Mixl1*, *Gata4*, *Cdx2*), and (D) ectoderm (*Sox3*, *Pax6*, *Tubb3*, *Nestin*). The *β-actin* gene was used as a control. For each gene, data were normalized to the mRNA level of wild-type ESCs. Shown are means ± SEM, n = 3 independent experiments.

used for the long-term study of miRNA functions and identified the meso-endoderm-promoting function of miR-294 during embryoid body differentiation.

miR-183/-182 Act Redundantly with the miR-290 Family to Promote the Self-Renewal and Pluripotency of ESCs

The let-7 family of miRNAs are highly enriched in somatic cells and rapidly upregulated during ESC differentiation (Landgraf et al., 2007). Interestingly, let-7c silences the self-renewal of $Dgcr8^{-/-}$ but not wild-type ESCs. The miR-290 family of miRNAs are reported to be responsible for blocking the differentiation-inducing function of let-7c (Melton et al., 2010). However, whether the miR-290 family of miRNAs are the only miRNAs required to block the function of let-7c is not clear. We investigated this question with miR-290$^{-/-}$ ESCs. Surprisingly, let-7c was not able to silence the self-renewal of ESCs lacking the miR-290 family (Figure S3), indicating that there are other miRNAs capable of blocking let-7c function in ESCs.

A

DISME miRNA pool

Dg8KO

U6 | miRNA

Blasticidin selection

Let-7c

Mix library

miRNA qPCR

B

Fold change(Let-7/Mock)

1000

100 — miR-182

10 — miR-672
miR-96
miR-93a miR-541
miR-293 miR-292-5p miR-183 miR-142
miR-291a
miR-20a
miR-19b

1 — miR-19a miR-135b miR-130 miR-127 miR-103

0.1

DISME miRNAs

* : P<0.01

C

Dg8KO+mock
200um

Dg8KO+Let-7c
200um

Dg8KO+Let-7c+miR-182
200um

Dg8KO+miR-26
200um

Dg8KO+miR-26+miR-182
200um

Dg8KO+miR-218
200um

Dg8KO+miR-218+miR-182
200um

D

Relative mRNA expression

Oct4
Sox2
Nanog

1.2
1.0
0.8
0.6
0.4
0.2

*
*
*

miR-182 - + - + - +
Let-7c   miR-26   miR-218

E

Relative mRNA expression

* : P<0.01

Oct4
Sox2
Nanog

2.0
1.8
1.6
1.4
1.2
1.0
0.8
0.6
0.4
0.2
0

*

Mock Let-7c   Mock Let-7c   Mock Let-7c   Mock Let-7c
WT   290KO   182KO   DKO

F

Mock   Let-7c

WT
200um   200um

DKO
200um   200um

G

OD 540nm

1.8
1.6
1.4
1.2
1.0
0.8
0.6
0.4
0.2

WT
290KO
182KO
DKO

0h   24h   48h

H

* : P<0.01

Number of GFP+ colonies

45
40
35
30
25
20
15
10
5

*

Control   miR-183~182

(legend on next page)

To identify miRNAs other than the miR-290 family that can block the function of let-7c, we designed a selection strategy based on DISME. The selection criterion is that $Dgcr8^{-/-}$ ESCs expressing miRNAs blocking let-7c will be enriched after introduction of let-7c. We first transfected $Dgcr8^{-/-}$ ESCs with a mixture of DISME vectors encoding miRNAs that are abundant in ESCs. After 5 days of blastici-din treatment to get rid of non-transfected cells, let-7c was transfected to enrich DISME of miRNAs that can promote the self-renewal and pluripotency of ESCs. After three rounds of selection, cells were collected for miRNA qPCR (Figure 5A). Interestingly, miR-182 was identified as the most significant hit. Moreover, its paralog miR-183 was also enriched in the selection as the third most significant hit (Figure 5B). miR-182 and miR-183 were produced from the miR-183–182 cluster, shared similar seed se-quences, were highly enriched in mouse ESCs, and downre-gulated during embryoid differentiation (Hadjimichael et al., 2016) (Figure S4A). We found that the expression of miR-182 and miR-183 was also higher in naive ESCs than primed EpiLCs (Gu et al., 2016) (Figure S4B), suggesting their function is associated with naive pluripotency. Furthermore, we verified the function of miR-182 and miR-183 in blocking let-7c with an miRNA mimics approach (Figures 5C, 5D, S4C, and S4D). Excitingly, miR-182 also suppressed two other differentiation-inducing miRNAs, including miR-26 and miR-218, in silencing the self-renewal of $Dgcr8^{-/-}$ ESCs, suggesting its general function against differentiation-inducing miRNAs (Figures 5C and 5D). To further test whether miR-182 and miR-183 act together with the miR-290 family of miRNAs to promote the self-renewal and pluripotency of ESCs, we constructed miR-290$^{-/-}$ and miR-183–182$^{-/-}$ double knockout mouse ESCs (DKO) using CRISPR/CAS9 (Figures S5A–S5E). Excitingly, while deletion of either miR-290 or the miR-183–182 cluster retained the ability to self-renew after the introduction of let-7c, the self-renewal of DKO ESCs was largely silenced by let-7c as demonstrated by qPCR analysis and alkaline phosphatase staining (Figures 5E and 5F). Therefore, miR-290 and miR-183–182 clusters functioned redundantly in promoting self-renewal and pluripotency in mouse ESCs. However, the precise pattern for the rescue of Oct4, Sox2, and Nanog expression by miR-182 was not exactly the same as miR-294 (Figure S5F), suggesting the two classes of miRNAs function through different mechanisms. In addition, DKO ESCs grew much slower than wild-type or single knockout ESCs (Figure 5G), suggesting possible redundancy of two miRNA families in regulating the proliferation of ESCs. Finally, consistent with its function in promoting ESC self-renewal and pluripotency, overexpressing miR-183–182 cluster increased the number of Oct4-GFP reporter-positive colonies ~1.7-fold in the reprogramming of mouse embryonic fibroblasts by Yamanaka factors (OCT4, SOX2, KLF4, and MYC) (Figure 5H). Taken together, DISME selection successfully identified miR-183–182 as another miRNA cluster that promotes self-renewal and plu-ripotency in ESCs.

DISCUSSION

In summary, we established that DISME can stably express miRNAs in $Dgcr8^{-/-}$ cells. Previously, functional studies of miRNAs in $Dgcr8^{-/-}$ cells could only be performed with chemically synthesized miRNA mimics (Cao et al., 2015; Gu et al., 2016; Guo et al., 2015; Ma et al., 2015; Melton et al., 2010; Sinkkonen et al., 2008; Wang et al., 2008, 2013). Here, we showed that DISME can produce high enough levels of miRNAs that can almost fully rescue

Figure 5. DISME Screen Identifies the Redundant Function of the miR-183–182 Cluster of miRNAs in Promoting Self-Renewal and Pluripotency of ESCs to the miR-290 Cluster
(A) Design of the DISME miRNA screen to identify miRNAs blocking the differentiation-inducing function of let-7c in $Dgcr8^{-/-}$ ESCs.
(B) Scatterplot showing the enrichment of each miRNA after screening by miRNA qPCR. Data were normalized to 5S rRNA and then to mock-transfected cells. Shown are means ± SD, n = 3 independent experiments.
(C) Representative images of alkaline phosphatase staining of $Dgcr8^{-/-}$ ESCs transfected with let-7c, miR-26, miR-218 mimics alone, or in combination with miR-182 mimics.
(D) qRT-PCR analysis of Oct4, Sox2, and Nanog. The β-actin gene was used as a control. For each gene, data were normalized to the mRNA level of mock-transfected $Dgcr8^{-/-}$ ESCs. Shown are means ± SD, n = 3 independent experiments.
(E) qRT-PCR analysis of Oct4, Sox2, and Nanog in wild-type, miR-290$^{-/-}$, miR-183–182$^{-/-}$, and double knockout ESCs. The β-actin gene was used as a control. For each gene, data were normalized to the mRNA level of mock-transfected wild-type ESCs. Shown are means ± SD, n = 3 independent experiments.
(F) Representative images of alkaline phosphatase staining of wild-type and double knockout ESCs after mock or let-7c transfection.
(G) Growth curve for wild-type, miR-290$^{-/-}$, miR-183–182$^{-/-}$, and double knockout ESCs by MTT assay. Shown are means ± SD, n = 6 independent experiments.
(H) Reprogramming assay. Oct4-GFP MEFs were infected with retroviruses expressing Yamanaka factors (OCT4, SOX2, KLF4, and MYC) plus control or miR-183–182 cluster, and the number of GFP-positive colonies were counted on day 15 after virus infection. Shown are means ± SD, n = 12 independent experiments.
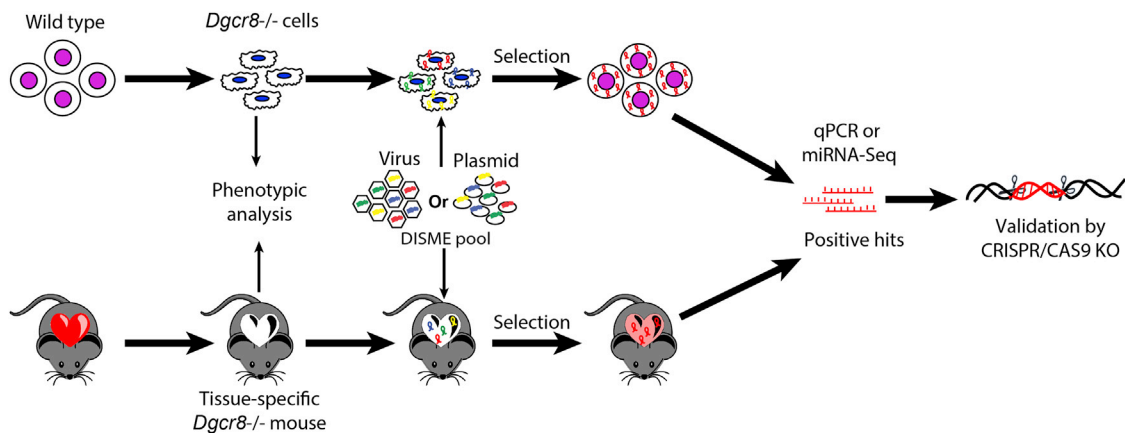
Figure 6. Summary Figure for the Design of the DISME Screen in *Dgcr8* Knockout Cell Lines or Tissues

defects of $Dgcr8^{-/-}$ cells in proliferation, gene expression, and differentiation. Therefore, DISME provides an alternative and cost-efficient approach to study miRNA functions in $Dgcr8^{-/-}$ cells. Two significant advantages of DISME versus miRNA mimics include its application in the study of long-term function and genetic selection of miRNAs (Figure 6) in $Dgcr8^{-/-}$ cells. Taking advantage of DISME, we found that miR-294 played a role in driving the formation of mesoderm and endoderm lineages. In addition, we identified an miR-182 cluster of miRNAs acting redundantly with an miR-290 cluster in promoting the self-renewal and pluripotency of ESCs. Together, our study demonstrates the applicability of DISME for long-term functional studies and genetic selection of miRNAs in $Dgcr8^{-/-}$ cells.

How the miR-182 family of miRNAs promotes self-renewal is not clear. The seed sequence of miR-182 is significantly different from that of miR-294. In addition, miR-294 but not miR-182 increased the proliferation rate of $Dgcr8^{-/-}$ ESCs (Wang et al., 2008). In future, knockout and DISME strategies should be used to elucidate the functions of miR-182 and miR-294 families in the differentiation of ESCs and during early embryonic development. Moreover, identification of functional mRNA targets of miR-182 and miR-294 will likely contribute to the understanding of redundant and non-redundant functions of these two miRNA families. Likewise, how miR-294 promotes the formation of meso- and endoderm is also not clear. Future work should focus on dissecting the function of miR-294 families at different stages of meso- and endoderm differentiation. This may be achieved through a conditional knockout strategy using tissue-specific Cre recombinase. In addition, screening for the mRNA targets of miR-294 that are responsible for mesoderm and endoderm lineages should be performed in $Dgcr8^{-/-}$ ESCs. Identification of these functional targets might reveal important

mechanistic insights on the early differentiation of meso-derm and endoderm lineages.

In the current design of DISME, the 5′ end of miRNAs is guaranteed to be the same as endogenous miRNAs by the loop-counting rule; however, miRNAs expressed by DISME differ by a few nucleotides from endogenous miRNA at their 3′ ends due to the termination sequence of Pol III. This is generally appropriate since the function of miRNAs largely depends on its 5′ end sequence, particularly the seed sequence (Bartel, 2009; Doench and Sharp, 2004; Lewis et al., 2003). However, in certain rare cases, the 3′ end sequence may play a role in target recognition and lead to different functional consequences. In these rare cases, to produce miRNAs with exactly the same sequences as endogenous miRNAs, future design may consider fusing an HDV-ribozyme downstream of the DISME construct to allow precise cleavage at the 3′ end of the miRNA sequence (Kuo et al., 1988; Sharmeen et al., 1988).

Intercrossing the $Dgcr8^{flox/flox}$ mouse line with mouse lines expressing tissue-specific promoter-driven Cre recombinase provides the means to study the function of miRNAs in specific tissue development or disease. Using this strategy, miRNAs were reported to be essential for the development or disease progression in a variety of tissues, including skin (Yi et al., 2009), the immune system (Bezman et al., 2010; Steiner et al., 2011), vascular smooth muscle (Chen et al., 2012), adipocytes (Kim et al., 2014), heart (Rao et al., 2009), kidney (Bartram et al., 2015), and brain (Hsu et al., 2012; Lin et al., 2015). However, a lack of approaches to stably express miRNAs in $Dgcr8^{-/-}$ cells has prevented identification of the exact miRNAs responsible for the defects uncovered by conditional $Dgcr8$ knockout mouse models. By adopting DISME into appropriate virus-based vectors, we expect that DISME will help accelerate the discovery of important miRNAs in normal function and disease progression of different tissues.

EXPERIMENTAL PROCEDURES

Plasmids and Vector Construction

miRNA sequences were cloned downstream of a U6 promoter in a *piggybac* vector that contains a blasticidin resistance gene driven by human *GAPDH* promoter. We used an 18 nt sequence from the 5′ end of miRNAs to design oligonucleotides ("N1_N18" is 18 bp of the miRNA sequence, while "R1_R18" is the reverse complementary sequence of "N1_N18"). Four oligos were synthesized by Invitrogen for each miRNA constructs: Oligo1: 5′-T-N1_N18-CTCC TGCTAC-3′; Oligo2: 5′-TGGGTCAGGGTAGCAGGAG-R1_R18-C-A-3′; Oligo3: 5′-TCGAGAAAAAAG-N1_N18-CTTGGGCTAC-3′; Oligo4: 5′-CCTGACCCAGTAGCCCAAG-R1_R18-CTTTTTTC-3′. To make the miRNA construct, these oligos were first phosphorylated with T4 PNK (NEB, M0201), then annealed at 95°C for 5 min and at room temperature for 1 hr. Annealed oligos were finally ligated into HpaI- and XhoI-digested *piggyBac* vectors. The sequences for oligos to generate miRNA expression plasmids can be found in Table S1.

Cell Culture, Plasmid Transfection, and Alkaline Phosphatase Staining

Wild-type and *Dgcr8*$^{-/-}$ ESCs were cultured on gelatin or irradiated mouse fibroblasts as reported previously (Wang et al., 2008). Approximately 1 day after plating, miRNA expression plasmids were transfected into cells, along with PBase expression plasmids using Lipo3000 (Life Technologies). After transfection, cells were treated with 10 mg/mL blasticidin S (Gibco) for 4 days. After that, cells were treated with TRIzol for RNA extraction or plated at single-cell density for colony picking. For alkaline phosphatase staining, cells were fixed with 4% paraformaldehyde for 10 min at room temperature, then stained for alkaline phosphatase (Vector Laboratories) following the manufacturer's protocol.

Small RNA Deep Sequencing and Data Analysis

Small RNAs libraries were generated using NEBNext small RNA library Prep Set for Illumina (E7330) and NEBNext multiplex oligos for Illumina (E7335) according to the manufacturer's instructions. Libraries were sequenced using the Illumina HiSeq2500. After trimming the adapters, the remaining sequence reads were matched to the miRBase r19 miRNA stem-loop sequences by Bowtie. Then the unmatched reads were rematched to rRNA, tRNA, small nucleolar RNA (snoRNA), repeats, intron, and mRNA. In each step, reads with zero or one mismatch were retained and the unmatched sequences were rematched in the next step. The "–best –strata" options were specified to allow mismatches and favor high-quality alignments. Mouse ribosomal, tRNA, and snoRNA sequences were extracted from Ensembl (Mus_musculus.GRCm38.69.ncrna.fa). Repeats, introns, and mRNAs were extracted from UCSC Tables (mm9). The miRNA expression profile was obtained according to the criterion described previously (Gu et al., 2016).

qRT-PCR and miRNA RT-PCR

RNA was extracted using TRIzol (Roche) and quantified by Biodropsis BD2000. Around 500 ng of RNA was reverse transcribed with a first-strand cDNA synthesis kit (Vazyme). qPCR was performed on ABI Step One Plus (Applied Biosystems). For miRNA qPCR, RNA samples were first polyadenylated with poly(A)polymerase and then reverse transcribed using a modified oligo-dT primer as described previously (Gu et al., 2016). Sequences for primers are listed in Table S2.

Embryoid Body Formation

Undifferentiated mESCs were first cultured in standard medium. Embryoid bodies were generated in low-attached dishes containing leukemia inhibitory factor (LIF)-free medium. The medium was changed every other day. RNA was extracted at day 0, 8, and 16 of differentiation and analyzed by RT-qPCR.

Cell Proliferation Assay and Cell-Cycle Analysis

Cells were plated at 4,000 cells per well in 96-well plates, incubated for 0, 24, and 48 hr before MTT (3-[4,5-dimethylthiazol-2-yl]-2,5-diphenyltetrazolium bromide) assay. Stock solution was added to a final concentration of 1 ng/μL. After incubation at 37°C for 3 hr, the MTT solution was removed, and 100 μL of DMSO was added to dissolve the precipitate. Absorbance was recorded at 540 nm using a MultiskanFC (Thermo Scientific). Cell-cycle analysis was performed as described previously (Wang et al., 2008).

miRNA Cluster Knockout Strategy

To knock out miR-290 and the miR-183/182 cluster, a pair of guide RNA sequences for each locus were designed by http://crispr.mit.edu/. Knockout of miR-290 and miR-183–182 clusters was verified by genomic PCR and miRNA qRT-PCR. Guide RNA sequences and the primers used in the knockout experiments are listed in Table S3.

Somatic Cell Reprogramming

OG2 mouse embryonic fibroblasts (MEFs) bearing a transgenic *Oct4-GFP* reporter were isolated, cultured, and reprogrammed as previously described (Li et al., 2010). For reprogramming, ∼15,000–20,000 MEFs per well in 12-well plates were infected twice with retroviral supernatants expressing Yamanaka factors and the miR-183–182 cluster of miRNAs. After infection, MEFs were cultured in mouse ESC medium (DMEM supplemented with 15% fetal bovine serum [GIBCO], non-essential amino acids, sodium pyruvate, β-mercaptoethanol, penicillin/streptomycin and LIF). GFP-positive colonies were counted at day 15 after the first infection.

Statistical Analysis

The data are presented as means ± SD except where indicated otherwise. The two-tailed unpaired Student's t-test was used to determine statistical significance. A p value <0.05 was considered statistically significant.

SUPPLEMENTAL INFORMATION

Supplemental Information includes five figures and three tables and can be found with this article online at https://doi.org/10.1016/j.stemcr.2017.08.027.

REFERENCES

Amin, N.D., Bai, G., Klug, J.R., Bonanomi, D., Pankratz, M.T., Gifford, W.D., Hinckley, C.A., Sternfeld, M.J., Driscoll, S.P., Dominguez, B., et al. (2015). Loss of motoneuron-specific microRNA-218 causes systemic neuromuscular failure. Science *350*, 1525–1529.

Bartel, D.P. (2009). MicroRNAs: target recognition and regulatory functions. Cell *136*, 215–233.

Bartram, M.P., Dafinger, C., Habbig, S., Benzing, T., Schermer, B., and Muller, R.U. (2015). Loss of DGCR8-mediated microRNA expression in the kidney results in hydronephrosis and renal malformation. BMC Nephrol. *16*, 55.

Bezman, N.A., Cedars, E., Steiner, D.F., Blelloch, R., Hesslein, D.G., and Lanier, L.L. (2010). Distinct requirements of microRNAs in NK cell activation, survival, and function. J. Immunol. *185*, 3835–3846.

Cao, Y., Guo, W.T., Tian, S., He, X., Wang, X.W., Liu, X., Gu, K.L., Ma, X., Huang, D., Hu, L., et al. (2015). miR-290/371-*Mbd2-Myc* circuit regulates glycolytic metabolism to promote pluripotency. EMBO J. *34*, 609–623.

Chen, Z., Wu, J., Yang, C., Fan, P., Balazs, L., Jiao, Y., Lu, M., Gu, W., Li, C., Pfeffer, L.M., et al. (2012). DiGeorge syndrome critical region 8 (DGCR8) protein-mediated microRNA biogenesis is essential for vascular smooth muscle cell development in mice. J. Biol. Chem. *287*, 19018–19028.

Chendrimada, T.P., Gregory, R.I., Kumaraswamy, E., Norman, J., Cooch, N., Nishikura, K., and Shiekhattar, R. (2005). TRBP recruits the DICER complex to AGO2 for microRNA processing and gene silencing. Nature *436*, 740–744.

Denli, A.M., Tops, B.B., Plasterk, R.H., Ketting, R.F., and Hannon, G.J. (2004). Processing of primary microRNAs by the Microprocessor complex. Nature *432*, 231–235.

Doench, J.G., and Sharp, P.A. (2004). Specificity of microRNA target selection in translational repression. Genes Dev. *18*, 504–511.

Fischer, S., Handrick, R., Aschrafi, A., and Otte, K. (2015). Unveiling the principle of microRNA-mediated redundancy in cellular pathway regulation. RNA Biol. *12*, 238–247.

Gu, S., Jin, L., Zhang, Y., Huang, Y., Zhang, F., Valdmanis, P.N., and Kay, M.A. (2012). The loop position of shRNAs and pre-miRNAs is critical for the accuracy of dicer processing in vivo. Cell *151*, 900–911.

Gu, K.L., Zhang, Q., Yan, Y., Li, T.T., Duan, F.F., Hao, J., Wang, X.W., Shi, M., Wu, D.R., Guo, W.T., et al. (2016). Pluripotency-associated miR-290/302 family of microRNAs promote the dismantling of naive pluripotency. Cell Res. *26*, 350–366.

Guo, W.T., Wang, X.W., Yan, Y.L., Li, Y.P., Yin, X., Zhang, Q., Melton, C., Shenoy, A., Reyes, N.A., Oakes, S.A., et al. (2015). Suppression of epithelial-mesenchymal transition and apoptotic pathways by miR-294/302 family synergistically blocks let-7-induced silencing of self-renewal in embryonic stem cells. Cell Death Differ. *22*, 1158–1169.

Ha, M., and Kim, V.N. (2014). Regulation of microRNA biogenesis. Nat. Rev. Mol. Cell Biol. *15*, 509–524.

Hadjimichael, C., Nikolaou, C., Papamatheakis, J., and Kretsovali, A. (2016). MicroRNAs for fine-tuning of mouse embryonic stem cell fate decision through regulation of TGF-beta signaling. Stem Cell Reports *6*, 292–301.

Hammond, S.M. (2005). Dicing and slicing: the core machinery of the RNA interference pathway. FEBS Lett. *579*, 5822–5829.

Han, J., Lee, Y., Yeom, K.H., Nam, J.W., Heo, I., Rhee, J.K., Sohn, S.Y., Cho, Y., Zhang, B.T., and Kim, V.N. (2006). Molecular basis for the recognition of primary microRNAs by the DROSHA-DGCR8 complex. Cell *125*, 887–901.

Hasuwa, H., Ueda, J., Ikawa, M., and Okabe, M. (2013). miR-200b and miR-429 function in mouse ovulation and are essential for female fertility. Science *341*, 71–73.

He, L., Thomson, J.M., Hemann, M.T., Hernando-Monge, E., Mu, D., Goodson, S., Powers, S., Cordon-Cardo, C., Lowe, S.W., Hannon, G.J., et al. (2005). A microRNA polycistron as a potential human oncogene. Nature *435*, 828–833.

Hsu, R., Schofield, C.M., Dela Cruz, C.G., Jones-Davis, D.M., Blelloch, R., and Ullian, E.M. (2012). Loss of microRNAs in pyramidal neurons leads to specific changes in inhibitory synaptic transmission in the prefrontal cortex. Mol. Cell. Neurosci. *50*, 283–292.

Hutvagner, G., McLachlan, J., Pasquinelli, A.E., Balint, E., Tuschl, T., and Zamore, P.D. (2001). A cellular function for the RNA-interference enzyme Dicer in the maturation of the let-7 small temporal RNA. Science *293*, 834–838.

Jonas, S., and Izaurralde, E. (2015). Towards a molecular understanding of microRNA-mediated gene silencing. Nat. Rev. Genet. *16*, 421–433.

Kanellopoulou, C., Muljo, S.A., Kung, A.L., Ganesan, S., Drapkin, R., Jenuwein, T., Livingston, D.M., and Rajewsky, K. (2005).

Dicer-deficient mouse embryonic stem cells are defective in differentiation and centromeric silencing. Genes Dev. *19*, 489–501.

Kim, H.J., Cho, H., Alexander, R., Patterson, H.C., Gu, M., Lo, K.A., Xu, D., Goh, V.J., Nguyen, L.N., Chai, X., et al. (2014). MicroRNAs are required for the feature maintenance and differentiation of brown adipocytes. Diabetes *63*, 4045–4056.

Kuo, M.Y., Sharmeen, L., Dinter-Gottlieb, G., and Taylor, J. (1988). Characterization of self-cleaving RNA sequences on the genome and antigenome of human hepatitis delta virus. J. Virol. *62*, 4439–4444.

Landgraf, P., Rusu, M., Sheridan, R., Sewer, A., Iovino, N., Aravin, A., Pfeffer, S., Rice, A., Kamphorst, A.O., Landthaler, M., et al. (2007). A mammalian microRNA expression atlas based on small RNA library sequencing. Cell *129*, 1401–1414.

Lewis, B.P., Shih, I.H., Jones-Rhoades, M.W., Bartel, D.P., and Burge, C.B. (2003). Prediction of mammalian microRNA targets. Cell *115*, 787–798.

Li, R., Liang, J., Ni, S., Zhou, T., Qing, X., Li, H., He, W., Chen, J., Li, F., Zhuang, Q., et al. (2010). A mesenchymal-to-epithelial transition initiates and is required for the nuclear reprogramming of mouse fibroblasts. Cell Stem Cell *7*, 51–63.

Lin, H.P., Oksuz, I., Hurley, E., Wrabetz, L., and Awatramani, R. (2015). Microprocessor complex subunit DiGeorge syndrome critical region gene 8 (*Dgcr8*) is required for Schwann cell myelination and myelin maintenance. J. Biol. Chem. *290*, 24294–24307.

Liu, Z., Skamagki, M., Kim, K., and Zhao, R. (2015). Canonical MicroRNA activity facilitates but may be dispensable for transcription factor-mediated reprogramming. Stem Cell Reports *5*, 1119–1127.

Lujambio, A., and Lowe, S.W. (2012). The microcosmos of cancer. Nature *482*, 347–355.

Ma, Y., Yao, N., Liu, G., Dong, L., Liu, Y., Zhang, M., Wang, F., Wang, B., Wei, X., Dong, H., et al. (2015). Functional screen reveals essential roles of miR-27a/24 in differentiation of embryonic stem cells. EMBO J. *34*, 361–378.

Melton, C., Judson, R.L., and Blelloch, R. (2010). Opposing microRNA families regulate self-renewal in mouse embryonic stem cells. Nature *463*, 621–626.

Olive, V., Minella, A.C., and He, L. (2015). Outside the coding genome, mammalian microRNAs confer structural and functional complexity. Sci. Signal. *8*, re2.

Parchem, R.J., Moore, N., Fish, J.L., Parchem, J.G., Braga, T.T., Shenoy, A., Oldham, M.C., Rubenstein, J.L., Schneider, R.A., and Blelloch, R. (2015). miR-302 is required for timing of neural differentiation, neural tube closure, and embryonic viability. Cell Rep. *12*, 760–773.

Rao, P.K., Toyama, Y., Chiang, H.R., Gupta, S., Bauer, M., Medvid, R., Reinhardt, F., Liao, R., Krieger, M., Jaenisch, R., et al. (2009). Loss of cardiac microRNA-mediated regulation leads to dilated cardiomyopathy and heart failure. Circ. Res. *105*, 585–594.

Sharmeen, L., Kuo, M.Y., Dinter-Gottlieb, G., and Taylor, J. (1988). Antigenomic RNA of human hepatitis delta virus can undergo self-cleavage. J. Virol. *62*, 2674–2679.

Sinkkonen, L., Hugenschmidt, T., Berninger, P., Gaidatzis, D., Mohn, F., Artus-Revel, C.G., Zavolan, M., Svoboda, P., and Filipowicz, W. (2008). MicroRNAs control de novo DNA methylation through regulation of transcriptional repressors in mouse embryonic stem cells. Nat. Struct. Mol. Biol. *15*, 259–267.

Steiner, D.F., Thomas, M.F., Hu, J.K., Yang, Z., Babiarz, J.E., Allen, C.D., Matloubian, M., Blelloch, R., and Ansel, K.M. (2011). MicroRNA-29 regulates T-box transcription factors and interferon-gamma production in helper T cells. Immunity *35*, 169–181.

Tian, Y., Liu, Y., Wang, T., Zhou, N., Kong, J., Chen, L., Snitow, M., Morley, M., Li, D., Petrenko, N., et al. (2015). A microRNA-Hippo pathway that promotes cardiomyocyte proliferation and cardiac regeneration in mice. Sci. Transl. Med. *7*, 279ra238.

Wang, Y., Medvid, R., Melton, C., Jaenisch, R., and Blelloch, R. (2007). DGCR8 is essential for microRNA biogenesis and silencing of embryonic stem cell self-renewal. Nat. Genet. *39*, 380–385.

Wang, Y., Baskerville, S., Shenoy, A., Babiarz, J.E., Baehner, L., and Blelloch, R. (2008). Embryonic stem cell-specific microRNAs regulate the G1-S transition and promote rapid proliferation. Nat. Genet. *40*, 1478–1483.

Wang, Y., Melton, C., Li, Y.P., Shenoy, A., Zhang, X.X., Subramanyam, D., and Blelloch, R. (2013). miR-294/miR-302 promotes proliferation, suppresses G1-S restriction point, and inhibits ESC differentiation through separable mechanisms. Cell Rep. *4*, 99–109.

Yan, Y., Yang, X., Li, T.T., Gu, K.L., Hao, J., Zhang, Q., and Wang, Y. (2017). Significant differences of function and expression of microRNAs between ground state and serum-cultured pluripotent stem cells. J. Genet. Genomics *44*, 179–189.

Yi, R., Pasolli, H.A., Landthaler, M., Hafner, M., Ojo, T., Sheridan, R., Sander, C., O'Carroll, D., Stoffel, M., Tuschl, T., et al. (2009). DGCR8-dependent microRNA biogenesis is essential for skin development. Proc. Natl. Acad. Sci. USA *106*, 498–502.